THE INFLUENCE OF GRAVITY ON THE SOLIDIFICATION OF A DROP

Angel SANZ, José MESEGUER and Luis MAYO

Laboratorio de Aerodinámica, ETSI Aeronáuticos, Universidad Politécnica, 28040 Madrid, Spain

Received 2 June 1986; manuscript received in final form 3 September 1986

In this paper the influence of gravity on the solidification of a drop formed at the end of a rod is analyzed. Although similar studies (but ignoring gravity effects) already exist, a theoretical analysis including gravity effects allows one to improve the experimental procedure to measure on Earth relevant properties of crystals (mainly the receding contact angle ϕ_1) which are of importance in shaped crystal growth processes. One of the main results here obtained are the shapes of the solidified drops, which are strongly dependent on the value of ϕ_1. Therefore, fitting theoretical shapes to experimental ones is a way to perform accurate measurements of ϕ_1.

1. Introduction

The study of the solidification process of a molten drop formed at the end of a rod has, at least, a double interest: in crystal growth and in fluid dynamics. This configuration appears in the simplest experiment which can be designed to grow a crystal from its melt (in absence of a crucible) and to determine the receding contact angle at an advancing interface between the melt and the growing solid [1] (other configurations have been employed in receding contact angle measurements [2,3], but they seem to be more complex from both experimental and theoretical points of view); on the other hand, the solidification of a drop can be used to study the advance of a solid–liquid interface. Up to now, this problem has been analyzed leaving apart gravitational and other inertial forces [1] and, in spite of the simplifying assumptions introduced in the mathematical model, theoretical results are in agreement with experimental ones obtained aboard Skylab-IV and Spacelab-1 [4,5]. Some other theoretical models did not succeed in fitting experimental results because of inappropriate initial conditions [6].

In this paper, the influence of gravity on the solidification of a liquid drop, mainly on the external shape of the resolidified material, is analyzed. As far as we know, some attempts have been made in connection with this problem, but in such studies gravity effects are only qualitatively discussed [7] and clear results are not offered.

The interest of the model presented here rests on the capacity to analyze the experiments performed on Earth, thus circumventing the scarce opportunity of space experiments. However, experiments on Earth have their own drawbacks mainly due to the reduced size of the drops.

In the following, we have posed the shape problem of the solidification process (section 2) and presented numerical results (section 3); in section 4, some experimental results on the determination of the receding contact angle are included. Finally, in the appendix, an analysis of the final stage of the solidification process is made by means of an asymptotic approximation of the non-linear problem.

2. Shape problem

To study the successive shapes adopted by the solid-liquid system shown in fig. 1, consisting of solidified material and the liquid drop anchored to the solidification front, the following widely used assumptions [1,2,6,8,9] are introduced:

(1) The gravity field is directed along the symmetry axis of the supporting rod, which is assumed to

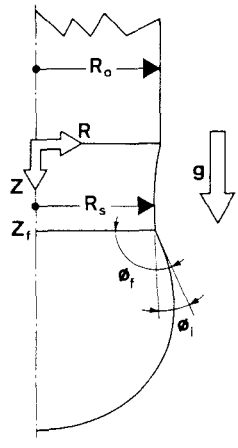

Fig. 1. Geometry and coordinate system for the drop crystallization problem: Z, R, axial and radial coordinates, respectively; Z_f, axial position of the solidification front; R_s, radius of the solidified crystal; R_0, rod radius; ϕ_f, angle between the solidification front and the liquid–gas interface; ϕ_i, receding contact angle.

be of circular cross-section. Then, the liquid–gas interface will be axisymmetric.

(2) The solidification front remains flat; therefore, the shape and thermal problems become decoupled. This hypothesis is confirmed by experiments reported below.

(3) The deformations produced by inner motions of the melt are negligible.

(4) The receding contact angle, ϕ_i, is assumed to be constant during the solidification process.

(5) Volume variations due to temperature differences are not accounted for. The volume variation at the phase change is assumed to happen suddenly at the solidification front.

As a consequence of hypothesis (2), the variation with time of the front position does not appear in the shape problem because it is decoupled from the thermal problem, which describes such variation.

Under these assumptions, the solidification process is characterized by the conservation of two variables at the solidification front $Z = Z_f$ (see fig. 1): the receding contact angle and the total mass [1],

$$\mathrm{d}R_s/\mathrm{d}Z = \tan\left(\phi_f - \phi_i - \tfrac{1}{2}\pi\right), \tag{1}$$

$$\mathrm{d}V/\mathrm{d}Z = -\pi\rho R_s^2, \tag{2}$$

where R_s is the radius of the solid, Z the axial coordinate, V the volume of the remaining liquid drop, ϕ_f the angle between the liquid interface and the solidification front and $\rho = \rho_S/\rho_L$ is the solid to liquid density ratio (at the melting point).

The appropriate initial conditions are

$$R_s(0) = R_0, \quad V(0) = V_0, \tag{3}$$

where R_0 is the radius of the supporting rod. Introducing $r_s = R_s/R_0$, $z = Z/R_0$ and $v = V/R_0^3$, the above expressions become

$$\mathrm{d}r_s/\mathrm{d}z = \tan\left(\phi_f - \phi_i - \tfrac{1}{2}\pi\right), \tag{4}$$

$$\mathrm{d}v/\mathrm{d}z = -\pi\rho r_s^2, \tag{5}$$

with

$$r_s(0) = 1, \quad v(0) = v_0. \tag{6}$$

In absence of gravity, ϕ_f depends only on $\alpha = v/r_s^3$ [1]. If gravity is considered, ϕ_f depends also on a new parameter, the Bond number $\mathrm{Bo} = \rho_L g R_s^2/\sigma = \mathrm{Bo}_0 r_s^2$, where g is the acceleration of gravity, σ is the liquid surface tension and Bo_0 is the initial value of the Bond number. As the method to calculate ϕ_f for given values of α and Bo is well known (for instance, see ref. [10]), no additional details are presented here.

3. Numerical results

The system of eqs. (4) and (5) with conditions (6) has been integrated by using a fourth order Runge–Kutta method. For instance, the solidified shapes corresponding to particular pendant and sessile drop configurations (in the case of silicon, $\rho = 0.93$, $\phi_i = 11°$) are shown in fig. 2. The parameters which characterize the solidification process are the material properties, ρ and ϕ_i, together with initial conditions, Bo_0 and α_0 ($\mathrm{Bo}_0 > 0$ means a pendant drop). Concerning the shape problem, the stability of the liquid drop remaining at the solid front during the solidification process de-

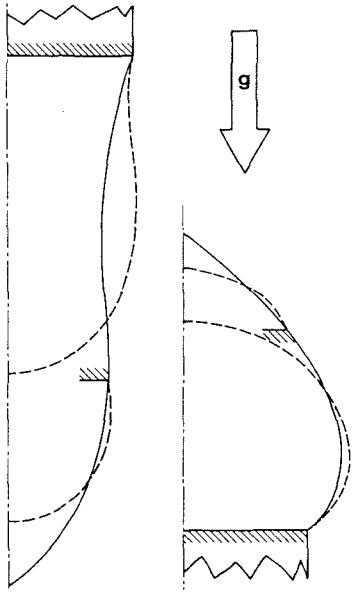

Fig. 2. Influence of gravity on the solidified shape (solid line) of a silicon crystal ($\phi_i = 11°$, $\rho = 0.93$) growing from a drop. These shapes have been obtained numerically from eqs. (4) and (5) in the case $v_0 = 6.8$ and $|Bo_0| = 0.7$. Initial and intermediate liquid interface shapes (dashed lines) are also shown.

pends on the values of the initial conditions Bo_0 and α_0. The process is stable when the liquid remains anchored to the solidification front and unstable when the drop breaks (unstable pendant drop) or "pours" over the edge of the solid (unstable sessile drop).

For a given material, any solidification process can be represented as a curve in the stable region of the (Bo, α) plane, as shown in fig. 3 for the case of silicon (details on the stability limits of both pendant and sessile drops can be found in refs. [11,12]). Concerning fig. 3, the following points are of interest.

Since a point (Bo, α) defines univocally the shape of a liquid drop, the subsequent evolution from each point is also unique, so that the different solidification curves cannot cross each other, except perhaps at the end.

There exists minimum values of initial conditions (Bo_m, α_m) given by the condition $\phi_f(Bo_m, \alpha_m) = \phi_i$, for which $dr_s/dz = -\infty$ at the start of the process; initial points below that curve represent configurations which would violate the flat solidification front hypothesis. In the case of silicon, ($\phi_i = 11°$), the curve $\phi_f = \phi_i$ is very close

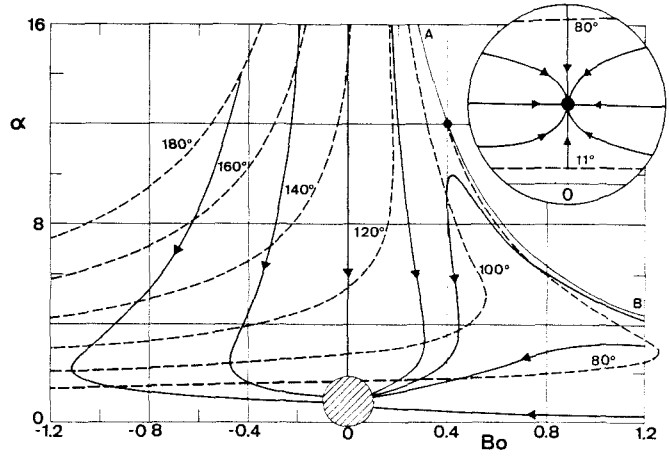

Fig. 3. Typical solidification evolutions (solid lines) calculated by solving eqs. (4) and (5) in the case of silicon ($\phi_i = 11°$, $\rho = 0.93$). Dashed lines indicate the angle of the liquid–gas interface ϕ_f at the drop support. Line AB and $\phi_f = 180°$ correspond to stability limits for pendant and sessile drops, respectively. Details concerning the final stage of the solidification process are shown in the insert.

to the Bo axis ($\alpha \ll 1$) and an approximate expression can be deduced (see eq. (A.2)). This region of small volume does not seem to be of great interest, and is too difficult to be experimentally attained except at the end of solidification.

All stable evolutions end at the same point $(0, \alpha_e)$, the end point of an evolution in zero gravity. This is the singular point of the system of eqs. (4) and (5), which will be analyzed below (see appendix). This analysis allows one to obtain the approximate shape of the solid and an estimation of ϕ_i from the slope of the solid at the apex.

In the case Bo > 0, there is a region near the stability limit inside which trajectories are attracted towards the stability limit. The size (width) of this region depends on ϕ_i and ρ. The larger ϕ_i, the larger the size of the region, the effect of ρ being the opposite, as shown in fig. 4. This region does not exist in the case of sessile drops (Bo < 0).

In fig. 3 also the curves ϕ_f = constant are shown;

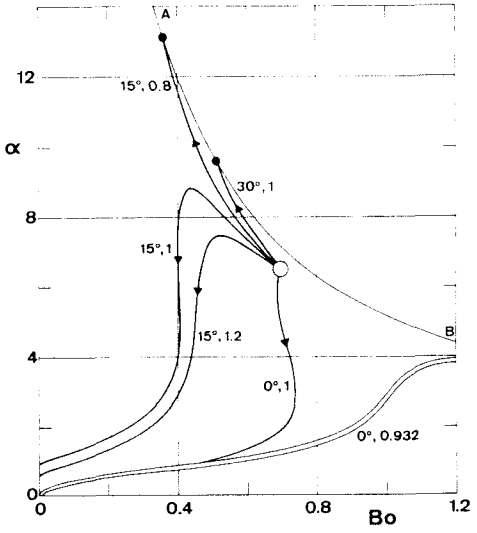

Fig. 4. Influence of the receding contact angle ϕ_i and the density ratio ρ in solidification evolutions. Numbers on the curves indicate the value of ϕ_i and ρ, respectively. The fringe in the lower part shows the evolution followed in the experiments (see also fig. 5). Line AB corresponds to the stability limit for pendant drops.

these curves are of help to explain the curvature of the trajectories. In the case of silicon, the large curvature changes occur near the curve $\phi_f = 101°$ because the solidified shape presents a maximum or a minimum when crossing this curve. In sessile configurations the shape can have one maximum (if $\phi_f(Bo_0, \alpha_0) > 101°$), whereas pendant configurations could have one maximum and one minimum. This is so because in the region Bo < 0 the ϕ_f curves are single-valued and $\phi_f(Bo, \alpha)$ monotonically decreases. In the Bo > 0 region these curves are double-valued.

4. Experiments

In order to make a simple illustration of the theoretical model, a few experiments have been performed. Water has been chosen as working fluid, for simplicity reasons. Although solidifications of both pendant and sessile drops have been performed, we only present the first case because, due to their elongated shapes, they are more suitable for comparison with theoretical shapes.

The setup consists of an aluminium rod (5 mm in diameter) which supports a liquid drop at one end, the second end being placed inside a reservoir. Once the drop is formed, liquid nitrogen is drawn in the reservoir so that heat from the rod is extracted by evaporation of nitrogen. Thus, when the melting temperature is reached at the drop support section, water begins to freeze and a solidification front starts to move along the drop. Successive front positions are shown in fig. 5, where the existence of a really flat front is demonstrated and it also shows a small translucid fringe ahead of it.

Comparison between theoretical and experimental results has been performed as follows: first, the initial and final forms have been digitized as shown in fig. 6. The volume of the initial drop has been directly calculated by numerical integration of digitized data obtaining $v_0 = V_0/R_0^3 = 3.92$. For this value of the dimensionless volume, the Bond number can be estimated by minimizing the distance between capillary curves (which, once the volume is known, only depends on Bo) and the experimental data as reported in [10], and the

value $Bo_0 = 1.22$ was obtained (which corresponds to a value of the surface tension of the order of 0.05 N m^{-1}).

Once the initial conditions are determined, the shape of solidified material is computed for several values of ϕ_i. The value $\rho = 0.932$ has been used in computations; this value, which has been obtained from measurements of the drop volume at initial and final stages of the solidification process, is 2% higher than the value quoted in the literature

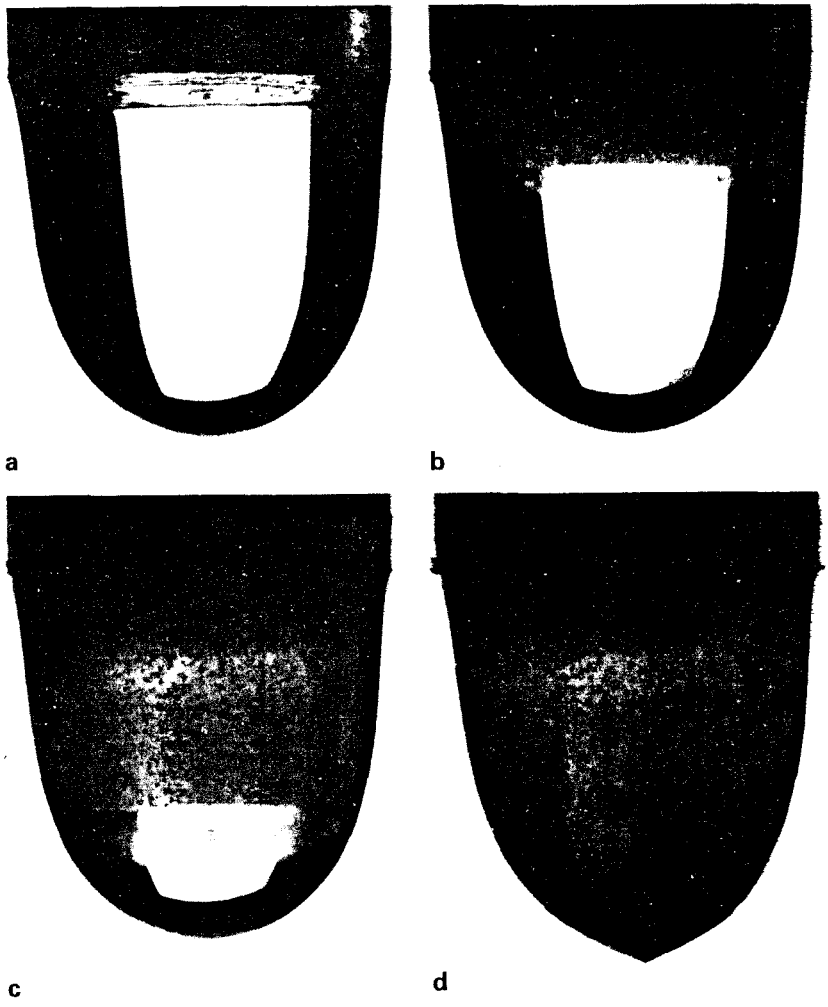

Fig. 5. Successive front positions for pendant solidification of a water drop from a cylindrical rod. Shadows correspond to the image of the background illumination.

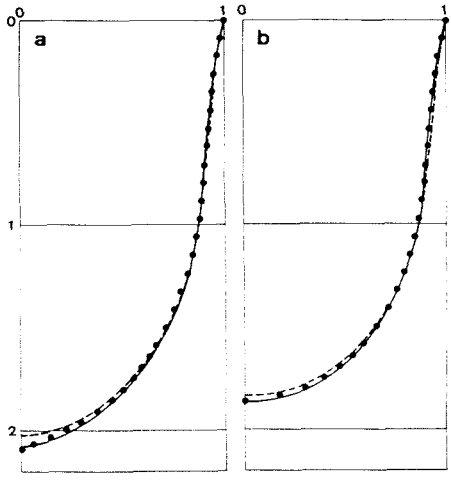

Fig. 6. Curves represented in (a) correspond to the solidified shape of the pendant drop shown in (b). Black circles indicate experimental points measured in photographs (fig. 5), whereas solid (dashed) line indicate theoretical results for $Bo_0 = 1.24$ (1.20) and $\phi_i = 0°$.

$\rho = 0.917$, and the difference could be due to digitization errors.

A method based on the least root-mean-square deviation between theoretical and experimental results has been employed to determine the value of ϕ_i. We define the standard deviation $S(\phi_i)$ as

$$S^2(\phi_i) = \frac{1}{N-1} \sum_{j=1}^{N} d_j^2, \tag{7}$$

where N is the number of experimental points taken into account and d_j is the minimum distance (made dimensionless with the rod radius) between an experimental point and the theoretical curve obtained for a given value of ϕ_i. The minimum value of $S(\phi_i)$ occurs at $\phi_i = 0°$, $S(0°) = 4.3 \times 10^{-3}$. The influence of ϕ_i is reported in table 1. The error in experimental measurements, obtained from magnified views, is of the order of 1% of the rod radius.

At the end of the solidified drop, an apex appeared (whose angle according to the appendix indicates $\phi_i \sim 5°$). This apex could be an spurious effect probably due to accumulation of impurities.

Table 1
Values of the standard deviation $S(\phi_i)$ between experimental and theoretical results for several values of the contact angle ϕ_i

$\frac{S(\phi_i) - S(0°)}{S(0°)}$	ϕ_i (deg)			
	0	0.5	1	2
0	0			
0.74	0.5			
2.14	1			
5.10	2			

In fact, although distilled water was employed, aluminium is known to be very difficult to clean. Other impurities could have come from the ambient air.

As the experimental evolution seems to be obey the above mentioned hypothesis, it can be deduced that the surface tension remains constant along the process except perhaps at the end, near the apex.

Comparison can be made with results from Surek and Chalmers [2]. In the final stage of their experiments the solidification process can be considered similar to that of a sessile drop. Samples F and H in fig. 3 of ref. [2] show the typical conical shape whose angle is predicted by the model presented here; from results reported in the appendix, the angle of the cone for silicon should be $90° - (\phi_f - \phi_i) = 50°$ (see fig. 2). Measured values in photographs of samples F and H of ref. [2] are 45° and 49° respectively.

5. Conclusions

In this paper we describe a theoretical model for the growing of a crystal from an axisymmetric drop of its melt including gravity effects. This model can be used to fit experimental results as a means to determine, in the case of a crystal, the receding contact angle ϕ_i. As account has been taken of gravity, comparison of theoretical results with experiments performed on Earth can be made, avoiding the restriction of the other previous model [1].

Main results presented here show the influence on the solidification process of the parameters

involved: the density ratio ρ and the receding contact angle ϕ_i, as well as initial conditions (the volume of the melt and the Bond number). Both sessile and pendant liquid configurations have been considered. In the latter case, the existence of a region close to the stability limit has been found where the remaining liquid drop, initially stable, becomes unstable. The size of this region depends on the values of ρ and ϕ_i.

Comparison between theoretical and experimental results predicting a receding contact angle $\phi_i = 0°$ for water has been presented.

The configuration proposed here to measure ϕ_i seems to be simpler that some others employed before [2,3] which additionally were not supported by a theoretical model accounting for gravity effects [2]. In fact, the variation of the value of ϕ_i reported in ref. [2] could be due to the influence of gravity on the meniscus shape, since, in the configuration they used to measure ϕ_i, the value of the Bond number is close to 0.4, which does not seem to be small enough to neglect gravity effects. This estimation of Bo is obtained by taking $R_0 = 3 \times 10^{-3}$ m, $\rho = 2530$ kg m^{-3} and $\sigma = 0.72$ N m^{-1}. In this case, R_0 is the typical radius of the molten zone at which measurements have been performed in ref. [2].

Finally, the asymptotic analysis shown in the appendix helps to understand the final steps of the solidification and allows one to obtain simple analytical expressions, valid for small values of the volume and the Bond number.

Appendix, Asymptotic solutions

The system of eqs. (4) and (5), written in variables Bo and α reads

$$\frac{d\alpha}{dz} = \frac{-\pi\rho + 3\alpha/\tan(\phi_f - \phi_i)}{(Bo/Bo_0)^{1/2}}, \tag{A.1a}$$

$$\frac{dBo}{dz} = -2\frac{(Bo\ Bo_0)^{1/2}}{\tan(\phi_f - \phi_i)}. \tag{A.1b}$$

An asymptotic analysis of the drop shape gives

$$\alpha = \tfrac{1}{4}\pi\phi_f(1 + Bo/24), \tag{A.2}$$

valid either for pendant or sessile drops, if $|Bo| < 1$ and $\alpha < 1$ (additional details can be obtained upon request from the authors). If $|Bo|$ and α are small enough, using eq. (A.2) and the approximation $\tan(\phi_f - \phi_i) \sim (\phi_f - \phi_i)$, the following expression results

$$\frac{d\alpha}{d\ Bo} = \frac{(4\rho - 3 - \frac{1}{6}\rho\ Bo) - \pi\rho\phi_i}{2\ Bo}. \tag{A.3}$$

Eq. (A.3) has a singular point at Bo = 0, $\alpha = \alpha_e = \pi\rho\phi_i/(4\rho - 3)$, corresponding to the end of all trajectories (see fig. 3), which obviously is the same as the end point of the evolutions in zero gravity condition [1] (the exact value of α_e is given by the solution of $\pi\rho\ \tan[\phi_f(0, \alpha_e) - \phi_i] = 3\alpha_e$).

To analyze the behavior of the different evolutions near this point, we can translate the origin to α_e, and stretch the coordinate Bo

$$\alpha = \alpha_e + \tilde{\alpha}, \tag{A.4a}$$

$$Bo = Lb, \tag{A.4b}$$

where $L = 6(4\rho - 3)^2/(\pi\rho^2\phi_i)$. Therefore, neglecting O $(\tilde{\alpha}b)$ terms, eq. (A.3) becomes

$$\frac{d\tilde{\alpha}}{db} = \frac{4\rho - 3}{2}\frac{\tilde{\alpha} - b}{b}. \tag{A.5}$$

This analysis is only valid if $\alpha < 1$ and $\alpha_e < 1$, so that $\rho > 3/(4 - \pi\phi_i)$. Also, owing to physical reasons, $\alpha \geqslant 0$. For instance, in the case of silicon this analysis gives $\alpha_e = 0.78$, whereas the value $\alpha_e = 0.79$ results from computations.

According to classical singular point theory, if $\rho > 3/4$ the singular point is a node and otherwise ($\rho < 3/4$) a saddle point. However, in this last case, the analysis is not valid because α is outside the applicability range ($\alpha_e < 0$). Thus, in the following we shall discuss the case $\rho > 3/4$ only. In this case, the solution of (A.5) is

$$\tilde{\alpha} = \frac{4\rho - 3}{4\rho - 5}b + \left(\tilde{\alpha}_0 - \frac{4\rho - 3}{4\rho - 5}b_0\right)\left(\frac{b}{b_0}\right)^{(4\rho - 3)/2}, \tag{A.6}$$

where $\tilde{\alpha}_0$ and b_0 are either the initial conditions or the coordinates of any point over the curve. A good understanding of the family of curves is given by the direction of asymptotes of (A.6). These are the particular solutions of (A.6) for which the integration constant is 0 or ∞, $\tilde{\alpha} = b(4\rho$

$-3)/(4\rho-5)$, and $b=0$. The curves (A.6) are tangent to one of the two asymptotes. As $\mathrm{d}\tilde{\alpha}/\mathrm{d}b \approx b^{(4\rho-5)/2}$, they are tangent to the α axis if $\rho < 5/4$ and to the other aymptote if $\rho > 5/4$. The sign of the slope of this asymptote depends on whether ρ is larger or smaller than $5/4$.

Once $\tilde{\alpha}(b)$ is determined, the approximate expression for $\mathrm{d}r_s/\mathrm{d}z$ is

$$\frac{\mathrm{d}r_s}{\mathrm{d}z} = -(\phi_f - \phi_i)^{-1} = -\left(\frac{4}{\pi}\tilde{\alpha} - \frac{4\rho-3}{\pi\rho}b + \frac{3\phi_i}{4\rho-3}\right)^{-1}, \qquad (A.7)$$

which can be integrated (since $b = r_s^2 \mathrm{Bo}_0/L$) to obtain

$$z_e - z = \left[\tilde{\alpha}_0 - \frac{2}{3}\frac{\rho^2\phi_i\,\mathrm{Bo}_0}{(4\rho-3)(4\rho-5)}\right]\frac{r_s^{4\rho-2}}{4\rho-2} + \frac{5}{18}\frac{\rho\phi_i\,\mathrm{Bo}_0}{(4\rho-3)(4\rho-5)}r_s^3 + \frac{3\phi_i}{4\rho-3}r_s. \qquad (A.8)$$

The slope $\mathrm{d}z/\mathrm{d}r_s$ at the end position, $z = z_e$, is $3\phi_i/(4\rho-3)$.

In the cases $\rho = 5/4$ or $\phi_i = 0$, eqs. (A.6) and (A.8) do not hold. However, suitable expressions can be deduced by performing the appropriate limits.

References

[1] A. Sanz, J. Crystal Growth 74 (1986) 642.
[2] T. Surek and B. Chalmers, J. Crystal Growth 29 (1975) 1.
[3] A. Wenzl, A. Fattah and W. Uelhoff, J. Crystal Growth 36 (1976) 319.
[4] H.U. Walter, AIAA Paper No. 74-1241 (1974).
[5] H. Koelker, in: Material Sciences under Microgravity, Results of Spacelab-1, ESA SP-222 (1984) p. 169.
[6] H. Rodot, M. Hamidi, J. Bourneix, A.S. Okhotin, I.A. Zoubridshi, V.T. Kriapov and E.V. Markov, J. Crystal Growth 52 (1981) 478.
[7] E.H. Zetterlund and H. Fredrikson, Mater. Letters 1 (1982) 127.
[8] T. Surek, S.R. Coriell and B. Chalmers, J. Crystal Growth 50 (1980) 21.
[9] W. Bradsley, F.C. Frank, G.W. Green and D.T.J. Hurle, J. Crystal Growth 23 (1974) 341.
[10] C. Huh and R.L. Reed, J. Colloid Interface Sci. 91 (1983) 472.
[11] D.H. Michael and P.G. Williams, Proc. Roy. Soc. (London) A354 (1977) 127.
[12] J.F. Padday and A.R. Pitt, Proc. Roy. Soc. (London) A275 (1973) 489.